PROCEEDINGS OF THE INTERNATIONAL CONFERENCE NANOMATERIALS: APPLICATIONS AND PROPERTIES
Vol. **1** No 2, 02NFC25(4pp) (2012)

The Influence of Annealing Thermal on the Properties of Au:TiO_2 Nanocomposite Film

A. Marin[1], D. Munteanu[1], C. Moura[2]

[1] *Department of Materials Science and Engineering, "Transilvania" University, 500036 Brasov, Romania*
[2] *Centro de Física, Universidade do Minho, 5710-057 Braga, Portugal*

(Received 23 June 2012; revised manuscript received 09 July; published online 10 August 2012)

Two sets of nanocomposite films consisting of different atomic concentrations of Au dispersed in a TiO_2 dielectric matrix were deposited by DC reactive magnetron sputtering, and subjected to several annealing tratament in vacuum, for temperatures ranging from 300 to 800 ^{0}C. The obtained results show that the structure and the size of Au clusters, together with the matrix crystallinity, changed as a result of the annealing As a result of these structural variations the film optical properties were modified too. The optical changes, and the correspondent Surface Plasmon Resonance effect were confirmed by reflectivity and CIELab colour measurements. XRD analysis confirmed the presence of gold in all the samples, and the crystallization of the TiO_2 matrix for the samples annealed at temperatures above 400^{0}C. With further increase of the annealing temperature, there is a change from the TiO_2 anatase phase into rutile-type structure. Simultaneously, the Au atoms are organized in crystalline nanoparticles (revealing an fcc-type structure, with the (111) preferential growth orientation).

Keywords: Thin films, Gold, Sputtering, Surface plasmon resonance.

PACS numbers: 81.15.Aa, 73.20.Mf

1. INTRODUCTION

Noble metal nanoparticles thin films are becoming an intensive area of research due to their interesting functional properties, including the possibility to have extensive colorations [1]. On the other hand, nanocomposite films consisting of noble metal nanoparticles, embedded in dielectric oxide matrixes, are being studied to be used in a wide range of applications, including those of catalysis, photo catalysis, sensors and novel optoelectronic devices [2]. One interesting feature is set when a noble metal is placed in a certain type of media, as it is the case of dielectric matrixes like that of titanium oxide. Titanium dioxide films are extensively used in optical thin-film device applications due to their appropriate optical properties, combined with high thermal and chemical stability in hostile environments [3, 4]. These films present good durability, a high transmittance in the visible spectral range, and a high refractive index, and thus are suitable for applications such as antireflection coatings, multilayer optical coatings (used as optical filters), optical waveguides, and others [5]. Some investigations indicated that very thin layers of noble metals on TiO2 surface can capture the photoinduced electrons or holes, eliminating the recombination of electron–hole pairs effectively and also extend the light response of TiO2 in the visible light region [6, 7]. Furthermore, nanoparticles of noble metals incorporated into a TiO_2 matrix are known to be able to improve its catalytic sensing and optical properties [7, 8].

In the particular case of the optical properties (the driving force in the present work), their behavior depends strongly upon the nanoparticles morphology [9]. The absorption spectrum is dominated by the resonant coupling of the incident field with quanta of collective conduction electron plasma oscillations, instead of monotonically increasing with wavelength. This resonance is called Surface Plasmon Resonance (SPR), and it is dependent on the concentration, size and shape of the metal clusters and, of course, on the dielectric properties of the surrounding medium [10, 11].

2. EXPERIMENTAL PROCEDURE

Two sets of Au:TiO_2 thin films (series A and B) were deposited onto silicon (100) and glass/quartz substrates by dc reactive magnetron sputtering, in a laboratory-sized deposition apparatus. For the depositions, a Ti target (99.6 % purity) was used, containing different amounts of incrusted Au pellets symmetrically incrusted in its preferential eroded zone. The number of Au pellets was varied in total amounts of 8 (series A) and 10 (series B), giving rise to two series of films with different chemical compositions. A constant dc current density of 100 Am^{-2} was applied. A mixture of argon and oxygen was injected with constant fluxes of 60 sccm and 10 sccm, corresponding to partial pressures of 0.3 Pa and 0.08 Pa, respectively. Samples were placed in a substrate holder, which was placed in a simple rotation mode (7 rpm). The substrates were biased (-50V) and the deposition temperature was set to a value of approximately 100 °C The temperature of the coated substrates was monitored with a thermocouple placed close to the surface of the substrate holder.

After film deposition, all samples were subjected to annealing experiments in vacuum. The annealing studies were carried out in a secondary vacuum furnace, after its evacuation to about 10 $^{-4}$Pa. The selected temperature range varied from 300 to 800 °C, and the isothermal time was fixed to 60 min, after the required heating time at 5 °C/min.

The structure and the phase distribution of the coatings were analyzed by X-ray diffraction (XRD), using a Philips PW1710 diffractometer (Cu-Kα radiation) operating in a Bragg–Brentano configuration. XRD patterns were deconvoluted, assuming to be Voigt functions to yield the peak position, integrated intensity. These parameters allow calculating the interplanar distance, preferential orientation and grain size. Optical properties (reflectance-transmittance) were characterized using a UV–vis-NIR Spectrophotometer (Shimadzu UV 3101 PC) in the spectral range from 250 to 800 nm. The color characterization were computed us-

ing a commercial MINOLTA CM-2600d portable spectrophotometer (wavelength range from 400 to 700 nm), using diffused illumination at a viewing angle of 8°. Color specification was computed under the standard CIE illuminant D65 (especular component excluded) and represented in the CIE 1976 L*a*b* (CIELab) color space [7, 12, 13].

3. RESULTS AND DISCUSSION

3.1 As-deposited film

The as deposited films, for the first set of samples, display a typical interference like behavior even for the in-situ doped films. This confirms the structural analysis since no Au nanoparticles are expected to induce the SPR effect after the deposition. Regarding the second as deposited films of samples, characterized by a higher quantity of gold embedded in the TiO_2 matrix, four broad peaks centered at 2θ of 38.2°, 44.4°, 64.7° and 77.3° fits quite well to the (111), (200),(220) and (311) reflections of the fcc-Au phase respectively.

For the as-deposited samples, all films exhibit broad and low intensity diffraction peaks.

3.2 Annealed coatings

After deposition all the films were submitted to annealing trataments in protective (vacuum) atmosphere up to 800 °C. The main idea was to promote some structural and morphological changes in the films, namely the change of the Au clusters size and their distribution on the dielectric TiO_2 surrounding medium and, consequently, to analyze the change of the optical properties of the films.

The influence of the Au clusters size embedded with in the dielectric matrix on the SPR activity was accessed, firstly, by reflectivity measurements, shown in Fig. 1. The reflectance spectrum for series A (Fig. 1a) noticed a slight decrease in reflectance with the increase of the thermal annealing treatment temperature. The reflectance spectra show a clear change from interference – like to an intrinsic behavior, with the increase of the annealing temperature. The change from one behavior to the other is revealed by the coating's surface tones that tend rapidly to a light purple color, when compared with the as-deposited and 300 °C annealed. The samples annealed at temperatures up to 600 °C reveal that the locations of the reflectivity minima are slightly shifting to lower wavelengths (437 nm at 300 °C to 413 nm for 600 °C).

Different reflectivity behavior was found for the samples from series B, characterized by a higher quantity of gold embedded in the TiO_2 matrix, if one compares the annealed samples with the as-deposited ones. As expected, the films present clear evidences that the Au content could be already in the upper limit to observe any optical interesting features, namely concerning its sensitivity to the SPR effects. The reflectivity increases up to the 600 °C sample (Fig. 1B), while the transmittance increases significantly starting with the 700 °C annealed sample.

Moreover, the optical behavior of the post-annealed series B is actually very similar to that obtained for "pure" gold. The higher reflectivity of the "pure" gold sample is due to its bulk morphology. As reported for "pure" TiO_2 the reflectivity of the as-deposited film does not show any unexpected optical behavior. Furthermore, it is also important to clarify that the "pure" TiO_2 films are known to show no remarkable optical behavior changes, even when heat treated at high annealing temperatures [14].

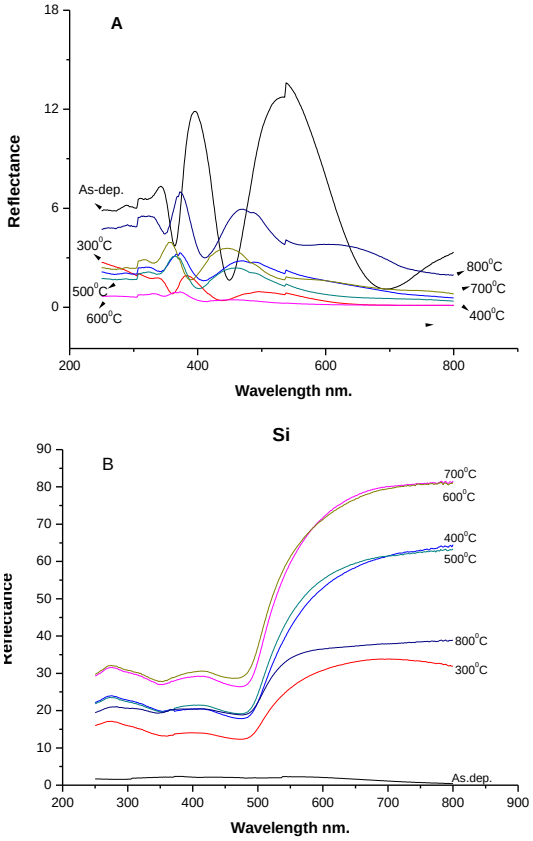

Fig. 1 – Variation of reflectivity as a function of annealing temperature (a) for series A, (b) for series B

The annealing process lead to the crystallization of the amorphous films, that is seen by the detection of signatures related with crystalline Au, followed by some crystallization of the TiOl matrix. The presence of Au, in sample A, is evidenced for annealing temperatures above 4000C, as it can be observed by the presence of the (111) peak, localized at 2θ = 38,26° as well as the (200) peak, at 2θ = 44,60° (Fig. 2A). At annealing temperatures above 300 °C, the TiO_2 phase changes from the anatase to the rutile structure.

A careful observation of the XRD patterns (Fig. 2B) for the samples B, which have a higher content of gold, shows that the initial broad Au (111) peak which starts to be detected at the as-deposided samples, becomes sharper with the annealing treatments,as are result of the grain growth probably due to the coalition of Au atoms. All the samples reveal some degree of crystalline gold as it can be observed by the presence of the peaks assigned to fcc (111), (200), (220) and (311) Au planes, localized at $2\theta \approx 38.1°$, $2\theta \approx 44.3°$, $2\theta \approx 64.67°$ and $2\theta \approx 77{,}54°$ respectively.

The Au clusters grow in size as the annealing temperature increase, which is followed by some crystallization of there remaining amorphous oxide dielectric matrix that occurs at an annealing temperature around 500 °C.

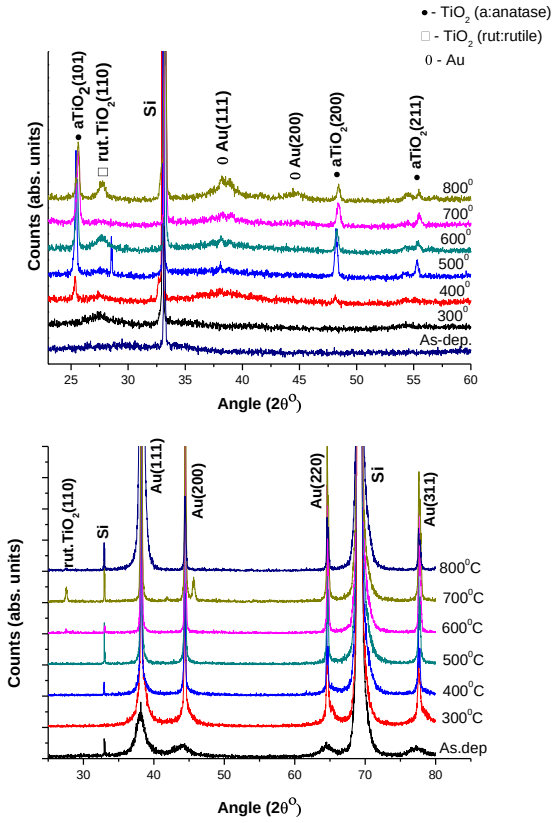

Fig. 2 – XRD diffraction pattern of Au:TiO_2 (a) sample series A as a function of the annealing temperature (b) sample series B as a function of the annealing temperature

It is also important to note that in the as-deposited sample only those Au peaks are seen, which leads to the conclusion that the gold is finely dispersed in the amorphous TiO_2 matrix. These four peaks become narrower and more intense with the increase of the annealing temperature.

Fig. 3 shows the results of the grow in size of the gold particles in the nanocomposite films, for the samples with higher content of gold, based on the integral breadth analysis of the XRD patterns. The Au particles sizes are increasing with the increase of annealing temperatures. The values of gold particles (clusters) size range from about 5 nm at as-deposited to approximately 77.3 nm at 700 °C. The SPR activity and the related changes on the optical properties are directly affected by this growth. Fig. 3 clearly illustrates the increasing on the Au particles size is continuous in this range of temperatures. Regarding the first set of samples, with low Au content, at temperature range between 400 °C and 500 °C there was noticed a significant increase in the gold particle grain size. The dimension of these gold particles is 35.7 nm for the 400 °C annealed sample and of 60.6 nm for the 500 °C annealed sample, followed by a decrease in grain size with increasing temperatures. The size of Au particles range from 40.8 nm at 600 °C to 4.8 nm at 800 °C.

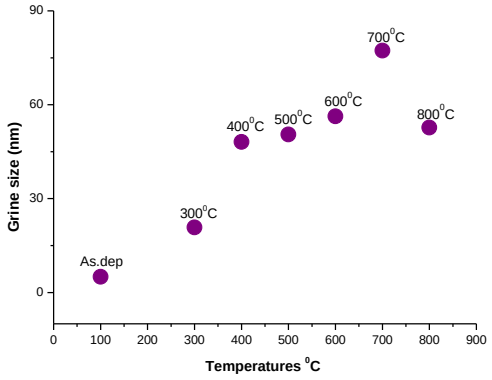

Fig. 3 – Variation of grain size of Au crystallites as a function of annealing temperature

It is clear that at Au concentrations between 30 at.% and 10 at.%, the SPR and color of the Au:TiO_2 thin films can be tuned by annealing treatments since they monitor the grain size and distribution of the Au clusters on the dielectric matrix [13].

4. CONCLUSIONS

The deposited films were subjected to annealing treat- ment at different temperatures.

The structural conditions are influenced by two different parameters, amount of Au gold doping the dielectric TiO_2 matrix and grain size of the Au nanoclusters that can be controlled by the annealing temperatures of the samples after the deposition.

Reflectivity percentages on the visible spectrum range and CIELab color values show a direct relation with the annealing temperature which is changing the grain size of gold clusters embedded in the dielectric matrix.

All the changes on the optical properties are consistent with the changes on crystal grain size studied on the XRD profiles.

To conclude, we have shown that the "one step" co-sputtering of a Ti-Au target, followed by an appropriate thermal treatment, is a useful way to produce composite TiO_2/Au films with adjustable nanostructure and, consequently, controllable SPR-related optical properties and color.

ACKNOWLEDGMENTS

This paper is supported by the Sectoral Operational Programme Human Resources Development (SOP HRD), ID76945 financed from the European Social Fund and by the Romanian Government.

REFERENCES

1. G. Walters, I. P. Parkin, *J. Mater. Chem.* **19**, 574 (2009).
2. M.G. Manera, J. Spadavecchia, D. Busoc, C. de Julian Fernandez, G. Mattei, A. Martucci, Mulvaney, J. Perez - Juste, R. Rella, L. Va sanelli, P. Mazzoldi, *Sensors Actuat. B* **132**, 107 (2008).
3. B. Karunagaran, R.T. Rajendra Kumar, D. Mangalaraj,

S.K. Narayandass, G. Mohan Rao, *Cryst. Res. Technol.* **37** 1285 (2002).
4. D. Mardare, P. Hones, *Mater. Sci. Eng. B* **68**, 42 (1999).
5. R.C. Adochitea, D. Munteanu, M. Torrell, L. Cunha, E. Alves, N.P. Barradas, A. Cavaleiro, J.P. Riviere, E. Le Bourhis, D. Eyidi, F. Vaz, *Appl. Surf. Sci.* **258**, 4028 (2012).
6. H. Y. Chuang, D. H. Chen, *Nanotechnology* **20**, 105704 (2009).
7. R.C. Adochite, M. Torrell, L. Cunha, E. Alves, N. P. Barradas A. Cavaleiro, J.P. Riviere, D. Eyidii, F. Vaz, *Optoelectronics and Advanced Materials* **5** No 1, 73 (2011).
8. N.P. Barradas, C. Jeynes, R.P. Webb, *Appl. Phys. Lett.* **71**, 291 (1997).
9. M. Torrell, R. Kabir, L. Cunha, M. Vasilevskiy, F. Vaz, A. Cavaleiro, E. Alves, *J. Appl. Phys.* **109**, 074310 (2011).
10. E. Hutter, J.H. Fendler, *Adv. Mater.* **16**, 1685 (2004).
11. V. Shutthanandan, Y. Zhang, S. Thevuthasan, L.E. Thomas, W.J. Weber, G. Duscher, C.M. Wang, *Nucl. Instrum. Meth. B* **242**, 448 (2006).
12. H. Ehrenreich, H. R. Philipp, *Phys. Rev.* **128**, 1622 (1962).
13. M. Torrell, P. Machado, L. Cunha, N. M. Figueiredo, J.C. Oliveira, C. Louro, F. Vaz, *Surf. Coat. Technol.* **204**, 1569 (2010).
14. H. Yoshida, H. Nasu, K. Kamiya, J. Matsuoka, *J. Sol-Gel Sci. Technol.* **9**(2), 145 (1997).